J. Membrane Biol. 177, 137–148 (2000)
DOI: 10.1007/s002320001107

The Journal of
Membrane
Biology

A Quantitative Model for the Dependence of Solute Permeability on Peptide and Cholesterol Content in Biomembranes

T.-X. Xiang*, J. Chen, B.D. Anderson*
Department of Pharmaceutics and Pharmaceutical Chemistry, University of Utah, Salt Lake City, UT 84112, USA

Received: 20 December 1999/Revised: 21 June 2000

Abstract. The influence of varying concentrations of a transmembrane peptide, gramicidin A (gA), and cholesterol (Chol) on the passive permeation of *p*-methylhippuric acid (MHA) and α-carbamoyl-*p*-methylhippuric acid (CMHA) across egg-lecithin membranes (EPC) has been investigated in vesicle efflux experiments. Incorporation of 0.25 volume fraction of gA in its nonchannel conformation increased the permeability coefficient (P_m) for CMHA by a factor of 6.0 ± 1.8 but did not alter P_m for MHA, a more lipophilic permeant. In contrast, incorporation of 0.26 volume fraction Chol with no added protein decreased the P_m values for both CMHA and MHA by similar factors of 4.2 ± 1.1 and 3.5 ± 1.2, respectively. A quantitative structure-transport model has been developed to account for the dependence of P_m on the membrane concentrations of gA and Chol in terms of induced changes in both membrane chain ordering and hydrophobicity. Chain ordering is assumed to affect P_m for both permeants similarly since they are comparable in molecular size, while changes in P_m ratios in the presence of gA or Chol are attributed to alterations in membrane hydrophobicity. Changes in lipid chain ordering were detected by monitoring membrane fluidity using fluorescence anisotropy of 1-[4-(trimethylamino)phenyl]-6-phenylhexa-1,3,5-triene incorporated into the membranes. The influence of additives on membrane hydrophobicity, which governs P_m ratios through effects on solute partitioning into the barrier domain, were rationalized within the framework of regular solution theory using solubility parameters as a measure of membrane hydrophobicity. Fits of the P_m ratios using the theoretical model yielded solubility parameters for gA and Chol in EPC membranes of 13.2 and 7.7 $(\text{cal/ml})^{1/2}$, respectively, suggesting that gA decreases the barrier domain hydrophobicity while Chol has a minimal effect on barrier hydrophobicity. After correcting for barrier domain hydrophobicity, permeability decrements due to membrane ordering induced by gA or Chol were found to exhibit a strong correlation with membrane order as predicted by free-surface-area theory, regardless of whether gA or Chol is used as the ordering agent.

Key words: Permeability coefficients — Gramicidin A — Cholesterol — Lipid bilayers — Solubility parameters — Fluorescence anisotropy — Regular solution theory

Introduction

Biomembranes are commonly described as fluid mosaics of proteins embedded within lipid bilayer matrices (Singer & Nicolson, 1972). Proteins and cholesterol (Chol) may comprise a substantial fraction of the overall mass of biomembranes, the composition of which may vary over a wide range depending on the type of membrane and on physiological or pathological conditions (Yeagle, 1992). For example, the protein content in Golgi membranes from rat liver is 1.21 mg per mg phospholipid while brush border membranes contain about 5.3 mg protein per mg phospholipid (Hauser et al., 1980; Daum, 1985). Cholesterol comprises about 30% of the total lipid mass in mammalian plasma membranes while more is found in lysosomes, endosomes, and Golgi (Yeagle, 1992).

Although the transport of many molecules of biological interest involves carriers and channel proteins, passive diffusion within biomembranes invariably occurs

* *Present address:* Division of Pharmaceutical Sciences, College of Pharmacy, University of Kentucky, Lexington, KY 40535, USA

Correspondence to: B.D. Anderson

for any small molecule upon its transfer from water into the membrane and is the predominant transport mechanism for many permeants. Because of this fundamental importance, extensive investigations of the passive permeation of small molecules have been undertaken in the past several decades using various model membranes, especially protein-free lipid bilayers (for examples, *see* (Haydon & Hladky, 1972; Finkelstein, 1976; Carruthers & Melchior, 1983; Walter & Gutknecht, 1986; Xiang, Chen & Anderson, 1992; Clerc & Thompson, 1995; Lande, Donovan & Zeidel, 1995; Xiang & Anderson, 1997; Paula, Volkov & Deamer, 1998). These studies have provided insight into the mechanisms by which the lipid composition (e.g., the acyl chain length, degree of unsaturation, and headgroup charges) and membrane physical state (e.g., phase structure, surface pressure, and temperature) affect molecular permeation processes.

The barrier function of biomembranes arises largely from the hydrophobicity and order of the membrane interior (Griffith, Dehlinger & Van, 1974; Seelig & Seelig, 1974; Subczynski et al., 1994; Xiang & Anderson, 1997). Cholesterol increases membrane order and decreases lipid hydration because of its rigid ring structure (Stockton & Smith, 1976; Simon, McIntosh & Latorre, 1982). Intercalation of Chol in gel-phase phospholipid membranes also shifts the barrier domain further into the acyl chain region (Xiang, Xu & Anderson, 1998). Biomembranes appear to differ markedly from protein-free lipid bilayers in their chemical selectivity to solute transport. For example, previous studies suggest that the barrier domain for transport across the blood-brain barrier closely resembles octanol in its selectivity to permeant structure (Rapoport, Ohno & Pettigrew, 1979; Levin, 1980). In contrast, the barrier domain within protein-free liquid-crystalline lipid membranes resembles that of a nonpolar solvent (e.g., decadiene) with negligible hydrogen bonding capacity (Walter & Gutknecht, 1986; Xiang et al., 1992; Xiang & Anderson, 1994). These studies have provided a qualitative description of solvent properties in biomembranes, but a quantitative approach is needed to describe changes in solute permeability across biomembranes varying in protein composition. While intensive efforts have been devoted to understanding the mechanisms for various protein-mediated transport processes, little is known regarding how strongly membrane proteins affect the basal permeability of small molecules, how these permeability changes depend on the nature, conformation, and concentration of membrane proteins, and the role membrane proteins play in regulating membrane hydrophobicity and order.

The relationship between molecular permeability and protein content is difficult to determine quantitatively in natural biomembranes where the distribution and structure of various membrane proteins are generally unknown. Therefore, in this study, we have explored the effects of a transmembrane peptide, gramicidin A (gA), as a model of the possible effects of proteins on solute basal permeability. Gramicidin A is a member of a large family of polypeptide antibiotics produced by *Bacillus brevis*, an aerobic soil bacterium. It consists of 15 amino acid residues, the sequence of which from the N- to C-terminus is formyl-Val_1-Gly_2-Ala_3-Leu_4-Ala_5-Val_6-Val_7-Val_8-Trp_9-Leu_{10}-Trp_{11}-Leu_{12}-Trp_{13}-Leu_{14}-Trp_{15}-ethanolamine with alternating L and D chirality (Anderson, 1984; Cornell, 1987). Gramicidin A is almost insoluble in water and can easily span certain bilayers in either a channel conformation where gA forms right-handed head-to-head single helical dimers with two monomers joined at their N-termini at the bilayer center or a nonchannel conformation where gA forms double-helical head-to-tail dimers depending on the organic solvent history for its incorporation into the membranes (Wallace, 1990; Killian, 1992). Thus, gramicidin A can be utilized as a model for the membrane-spanning part of intrinsic membrane proteins. Gramicidin A and its influence on membrane structure have been extensively studied using various spectroscopic and thermal methods (Cox et al., 1992; Koeppe, Killian & Greathouse, 1994; Muller, van Ginkel & van Faassen, 1995).

The influence of gramicidin A and cholesterol on the transport mechanisms of neutral and ionized α-X-*p*-methylhippuric acid analogues (XMHA) and neutral α-X-*p*-toluic acid (XTA) (X = H, Cl, OCH_3, CN, OH, COOH, and $CONH_2$) across phospholipid membranes has been investigated in previous studies by the authors (Xiang et al., 1998; Xiang & Anderson, 2000). Linear free energy relationships were established using various model solvents to explore the barrier hydrophobicity in the membranes. The barrier domains in gA- and Chol-containing membranes were found to be substantially more hydrophobic than octanol, thus establishing the location of the barrier domain as being beyond the hydrated headgroup region and eliminating transient water pores as a significant transport pathway. The addition of 10 mol% gA was found to decrease the hydrophobicity of the barrier domain from an environment resembling that of decadiene to that of a solvent possessing some degree of hydrogen-bond acceptor capacity (e.g., butyl ether) while the addition of 50 mol% Chol had a minimal effect on barrier domain hydrophobicity in liquid-crystalline membranes.

The aim of the present study is to develop a quantitative model to describe changes in solute permeability coefficients accompanying the incorporation of varying concentrations of gA or Chol into lipid bilayer membranes. Changes of membrane order and hydrophobicity in gA- and Chol-containing egg lecithin membranes and their effects on solute permeability have been evaluated by fluorescence anisotropy measurements using membrane-incorporated 1-[4-(trimethylamino)phenyl]-6-

phenylhexa-1,3,5-triene (TMA-DPH), fluorescence lifetime determinations using 12-(9-anthroyloxy) stearic acid (12-ANS), and permeability coefficients obtained from vesicle efflux studies for α-carbamoyl-*p*-methylhippuric acid (CMHA) and unsubstituted *p*-methylhippuric acid (MHA). The fluorophores in TMA-DPH and 12-ANS reside in the ordered lipid chain region (Podo & Blasie, 1977; Lentz, 1993), which is known to be the barrier domain for solute permeation across lipid membranes (Xiang et al., 1992; Xiang & Anderson, 1994). In the quantitative approach developed in this paper, changes in membrane order induced by gA or Chol influence solute permeability according to the predictions of free-surface-area theory, (Xiang & Anderson, 1997) where free surface areas can be obtained from TMA-DPH fluorescence anisotropy data. The model permeants chosen for this study have a similar molecular size but markedly different lipophilicities. Thus, changes in their *relative* permeability coefficients with added gramicidin A or cholesterol are sensitive to changes of membrane hydrophobicity rather than membrane order. Solubility parameters, derived from solution theory (Hildebrand & Scott, 1950), are employed as quantitative descriptors of membrane hydrophobicity. Though regular solution theory has been particularly successful in describing thermodynamic properties of dilute and relatively nonpolar solutions (Grant & Higuchi, 1990), its applicability to molecular transport in biomembranes has not been widely explored. The results presented herein demonstrate that the dependence of solute permeability coefficients on gA and Chol concentration in model membranes can be described quantitatively by considering the combined effects of membrane order and hydrophobicity.

Materials and Methods

Materials

L-α-lecithin-(phosphatidylcholine) (>99%) from egg yolk (EPC) and phosphatidic acid (PA) (>99%) were purchased from Avanti Polar Lipids (Pelham, AL). Cholesterol (99+%) was purchased from Sigma (St. Louis, MO). Gramicidin A was purchased from Fluka Chemical (Ronkonkoma, NY). All the phospholipids were stored in a freezer upon arrival. α-Carbamoyl-*p*-methyl-hippuric acid was synthesized in this laboratory as described elsewhere (Mayer, Xiang & Anderson, 2000). *p*-Methylhippuric acid (>98%, Sigma Chemical (St. Louis, MO) was used as received without further purification. 1-[4-(Trimethylamino)phenyl]-6-phenylhexa-1,3,5-triene (TMA-DPH) and 12-(9-anthroyloxy) stearic acid (12-ANS) were purchased from Molecular Probes (Eugene, OR). All other reagents were obtained commercially and were of analytical reagent grade.

Preparation and Characterization of Large Unilamellar Vesicles

Vesicle Preparation

Lipids (50–100 mg EPC, 3–6 mg PA, and/or Chol at varying volume fractions) were accurately weighed, dissolved in 25 mL chloroform in a test tube, and evaporated to a dry thin film under nitrogen. PA (5 mol%) was included in these membranes to reduce the rate of vesicle aggregation and thereby enhance vesicle stability (Cevc et al., 1988). LUVs containing up to 0.25 volume fraction of gA were prepared by adding an aliquot of a solution of gA in ethanol (1 mM) and evaporating the solvent under nitrogen. This method is known to incorporate gA into lipid membranes in a predominantly nonchannel conformation (Muller et al., 1995). The dried film was then left under vacuum for 12 hr to eliminate trace quantities of organic solvent. An aqueous solution containing $(1–2) \times 10^{-3}$ M permeant, 0.01 M buffer (phosphate or borate), 0.1 M NaCl, and 0.02 mM EDTA at a given pH was then added to yield a final total lipid concentration of 8–10 mg/ml. The dried lipid-peptide film was hydrated by repeated vortexing and shaking. The suspension formed was then extruded successively through 0.4, 0.2 and/or 0.1 μm polycarbonate filters (Nuclepore, Pleasanton, CA) to form predominantly large unilamellar vesicles (LUVs) with similar hydrodynamic diameters (Xiang & Anderson, 1995).

Dynamic Light Scattering

The vesicle hydrodynamic diameter, *d*, was determined in each vesicle sample by dynamic light scattering (DLS) measurements. The apparatus for DLS experiments consisted of a goniometer/autocorrelator (Model BI-2030AT, Brookhaven, Holtsville, NY) and an argon ion laser (M95, Cooper Laser Sonics, Palo Alto, CA) operated at 514.5 nm wavelength. A 30 μl aliquot of the LUV suspension was added to 2 ml of the same filtered buffer solution and placed in a clean glass test tube (13 × 75 mm). The sample was then placed in a temperature-controlled cuvette holder with a toluene index-matching bath. Autocorrelation functions were determined for a period of 100–500 sec with a 20–30 μsec duration at 90°C and analyzed by the method of cumulants.

Peptide Content Analysis

An analytical method developed previously (Xiang & Anderson, 2000) was employed to determine the gA concentration in the LUVs. The vesicles were lysed and diluted in methanol (1:2 v/v). The clear sample was then analyzed for gA by measuring absorbance at 280 nm (Cary 3E UV-Vis Spectrophotometer, Varian) and comparing to a standard curve of gramicidin A in methanol/water (1:2 v/v) and for phosphorus content by the method of Bartlett (Bartlett, 1959). Incorporation of gramicidin A into lipid membranes was verified by the failure to detect a significant amount of gA in the aqueous filtrate upon ultrafiltration of gA-containing LUVs.

Determination of Permeability Coefficients

The efflux transport method employed has been described in detail previously (Xiang & Anderson, 1998; Xiang & Anderson, 2000) and is therefore summarized below:

Gel Filtration

A size-exclusion column (Sephadex G-50, medium fractionation range, Sigma) in a 10 ml disposable syringe was equilibrated with the same buffer solution as that used to prepare the LUVs but without permeant. Aliquots (0.5–0.6 ml) of the permeant-loaded LUVs prepared above were transferred onto the column and eluted by centrifugation at two speeds (2 min at 300 × *g;* 1 min at 900 × *g*). Vesicles with entrapped permeant appearing in the void volume of the gel column well separated from the extravesicular permeant fraction were collected in a screw-capped 10-ml glass vial that was immediately placed in a 25°C

water bath. HPLC indicated an initial ratio of entrapped to extravesicular permeant concentration after size-exclusion chromatography on the order of 10^5.

Ultrafiltration

The efflux of permeant due to the concentration gradient created by gel filtration was determined by monitoring extravesicular permeant concentrations by HPLC. Aliquots (0.4 ml) of the LUVs obtained from gel filtration were taken at various time intervals and loaded onto a Centricon-100 filter (MWCO = 100,000; Amicon, Beverly, MA), centrifuged at 1,200 × *g* for 3–6 min and aliquots of the filtrate (*ca.* 100–200 μl) were subsequently analyzed. Total permeant concentrations in the LUVs were determined by lysing samples with a small amount of Triton X-100 (Sigma) prior to analysis.

Changes of the extravesicular permeant concentration with time were described by the following kinetic equation

$$\ln[(C_\infty - C_0)/(C_\infty - C_t)] = k_{obs}\, t \tag{1}$$

where C_0, C_t, and C_∞ are the extravesicular permeant concentrations at time 0, t, and at equilibrium, respectively, and k_{obs} is the apparent first-order rate constant.

$$P_m = k_{obs}(1 + 10^{pH - pK_a})V/A \tag{2}$$

Recent studies in the authors' laboratory have shown that the permeabilities of ionized MHA analogues are negligible in the pH range of interest (6.5–9.5) (Xiang & Anderson, 2000). Thus, the permeability coefficient for a neutral MHA permeant, P_m, can be obtained from the first-order rate constant, k_{obs}, via the above equation where K_a is the acid dissociation constant of the permeant and the ratio between the entrapped volume and surface area of the LUVs, V/A, is obtained from the vesicle hydrodynamic diameter, d ($V/A = d/6$).

HPLC Analyses

An HPLC system described previously (Xiang & Anderson, 2000) and a reversed-phase column packed with 5 μm Jupiter RP-C18 (Phenomenex, Torrance, CA) were used for the analyses of the samples taken during the transport experiments. The mobile phase contained 7–35 v/v% acetonitrile solvent depending on the analyte lipophilicity and 0.01 M phosphate buffer at pH = 3.0.

Fluorescence Anisotropy Measurements

The steady-state fluorescence anisotropy for TMA-DPH incorporated into lipid membranes was measured with a Greg 200 spectrofluorometer (ISS, Champaign, IL) in the photon counting mode using LUV samples prepared according to the procedures described above with final lipid and probe concentrations of 0.3 mM and 1 μM, respectively. The excitation was at 360 nm (300 W Xenon arc lamp, ILC Technology, Sunnyvale, CA) and the fluorescence emission was collected through a cut-on filter at 400 nm. The fluorescence intensities were collected through a polarizer oriented parallel ($I_\parallel$) or perpendicular ($I_\perp$) to the direction of the excitation polarization. The steady-state anisotropy, r_{ss}, was calculated as follows:

$$r_{ss} = \frac{(I_\parallel - I_\parallel^o) - G(I_\perp - I_\perp^o)}{(I_\parallel - I_\parallel^o) + 2G(I_\perp - I_\perp^o)} \tag{3}$$

where I^o measures the contribution from scattered light in the absence of probe and G is the grating correction factor. The temperature of the vesicle samples was maintained at 25°C by a circulating water bath (Techne, Princeton, NJ).

Fluorescence Lifetime Measurements

Fluorescence lifetimes for 12-(9-anthroyloxyl)-stearic acid (12-ANS) incorporated into lipid membranes (lipid and 12-ANS concentrations were 0.2 mM and 5 μM, respectively) and in hexadecane (at a 12-ANS concentration of 4 μM) were measured on an ISS K2 multifrequency phase and modulation fluorometer (ISS, Champaign, IL) equipped with a frequency synthesizer (Marconi Instruments, Allendale, NJ) and an ISS-ADC interface for data collection and analysis. Samples were excited by the 350 nm line of an argon ion laser. The phase shifts and modulation factors were determined at 12 different modulation frequencies between 10 and 150 MHz. The fluorescence emission was collected through a 390 nm cut-on filter. A nonlinear least-squares program from ISS (ISS187) was used to minimize the reduced χ^2 (the squared deviation between the observed and calculated phase shifts and demodulation factors) and calculate various lifetime components using single- or multi-exponential decay models. A solution of 1,4-bis[5-phenyl-2-oxazolyl]benzene (POPOP) in methanol (τ = 1.32 ns) was used as a reference.

Theoretical Section

According to the "barrier domain" permeability model (Xiang & Anderson, 1994, 1997), the lipid bilayer is viewed as a multilaminate assembly of distinctly different regions (i.e., the polar head groups, ordered acyl chains, and the relatively disordered hydrocarbon chain region in the center), with one region constituting the rate-limiting or barrier domain. The permeability coefficient for a given solute, P_m, can therefore be expressed as

$$P_m = \frac{K_{w-b}\, D_b}{d_b} \tag{4}$$

where $K_{w\to b}$ and D_b are the partition coefficient from water into and the diffusion coefficient in the barrier domain, respectively, and d_b is the thickness of the barrier domain. Supporting this permeability model are recent computer simulations by Marrink and Berendsen (1994, 1996) which have demonstrated distinctly different permeability properties in different regions of lipid membranes. The location of the barrier domain has been established to be the acyl chain region, the solvent properties of which resemble those in nonpolar hydrocarbons such as decadiene and hexadecene (Xiang & Anderson, 1994).

In contrast to the barrier domain model, the bulk solubility-diffusion model treats the lipid bilayer as a thin isotropic bulk solvent film and the permeability coefficient, P_o, is calculated as (Xiang & Anderson, 1997)

$$P_o = \frac{K_{w\to o}\, D_o}{d_o} \tag{5}$$

where $K_{w\to o}$ is the bulk solvent/water partition coefficient, D_o is the diffusion coefficient in the model solvent, and d_o is the overall membrane thickness. Because of the ordered nature of the barrier domain, P_m as defined in Eq. 4 is generally smaller than P_o predicted from the bulk solubility-diffusion permeability model, even when a model solvent is chosen which closely resembles the hydrophobicity of this domain (Xiang & Anderson, 1997).

Since D_o is determined mainly by the packing density of the medium and depends only weakly on medium polarity (Chan, 1983),

changes of membrane hydrophobicity in the presence of different amounts of transmembrane peptides/proteins and other membrane constituents are assumed to affect only the partition coefficient, $K_{w\to o}$. These changes are described here in the framework of regular solution theory (Hildebrand & Scott, 1950). According to this theory and in the limit of dilute solutions, $\log P_o$ can be expressed as

$$\log P_o = \log(D_o/d_o) + \frac{V_s}{2.303\mathrm{RT}}[(\delta_w - \delta_s)^2 - (\delta_m - \delta_s)^2] + \log(V_s/V_o) \quad (6)$$

where δ_w and δ_s are respectively the solubility parameters of water and the permeating solute, V_s and V_o are respectively the molar volumes of the solute and bulk solvent chosen as a model of the membrane, R is the gas constant, and T is the absolute temperature. The last term in Eq. 6 accounts for the transformation of solute concentration units from mole fraction to molarity which is applicable to $K_{w\to o}$ (Diamond & Katz, 1974). The bulk solvent chosen is assumed to have a molar volume similar to the effective molar volume of the membrane. The solubility parameter (δ_m) for membranes containing two different constituents can be calculated as follows (Bustamante & Selles, 1986)

$$\delta_m = (1 - \varphi_2)\delta_1 + \varphi_2\delta_2 \quad (7)$$

where δ_1 and δ_2 are the solubility parameters for the membrane components 1 and 2, respectively, and φ_2 is the volume fraction of component 2 in the membrane. In this analysis, EPC is assumed to be component 1 while component 2 is either gA or Chol.

We have previously introduced a correction factor to quantify the effects of lipid chain ordering on permeability (Xiang & Anderson, 1997). This permeability decrement factor, f_m, is defined as follows:

$$\log f_m = logP_m - logP_o \quad (8)$$

We have recently shown that, regardless of the membrane composition, phase structure, and temperature, the permeability decrement, f_m, is determined mainly by permeant size (cross-sectional-area A_s) and membrane mean free-surface-area, A_f (Xiang & Anderson, 1997, 1998), with the latter being intimately related to lipid order parameter, S_m (DeYoung & Dill, 1988; Nagle, 1993), as described in Eq. 9:

$$f_m = f_o \exp\left[-\lambda \frac{A_s}{A_o}\frac{(1 + 2S_m)}{(1 - S_m)}\right] \quad (9)$$

where f_o and λ are constants independent of solute size and membrane order parameter and A_o is the area per lipid in the crystal. Transmembrane peptides/proteins and other membrane components may alter both chain packing (e.g., S_m) and hydrophobicity (e.g., δ_m) with both S_m and δ_m being functions of the concentrations of these membrane components. Changes in membrane order with changes in membrane composition can be evaluated using fluorescence anisotropy, deuterium NMR, and other spectroscopic methods.

Combining Eqs. 6 and 8, the ratio of a given solute's permeability coefficient in a 2-component membrane (i.e., containing either gA or Chol with EPC) to that in a pure EPC membrane can be written as

$$\log(P_m/P_{EPC}) = \alpha_1\varphi_2 + a_2\varphi_2^2 + \log(V_{EPC}/V_o) + \log(f_m/f_{EPC}) \quad (10)$$

where

$$a_1 = \frac{2V_s}{2.303RT}(\delta_{EPC} - \delta_2)(\delta_{EPC} - \delta_s) \quad (11)$$

Table 1. Hydrodynamic diameters (d) of large unilamellar vesicles comprised of EPC, PA and different concentrations of gramicidin A or cholesterol

Vesicle composition (mol%)	d (nm)[a]	Extrusion procedure
EPC/PA/gA:		
95/5/0	177 ± 3	2 × 0.4 μm + 15 × 0.2 μm
94/5/1	183 ± 5	2 × 0.4 μm + 15 × 0.2 μm
93/5/2	178 ± 5	2 × 0.4 μm + 15 × 0.2 μm
91/5/4	189 ± 4	2 × 0.4 μm + 15 × 0.2 μm
88/5/7	183 ± 4	2 × 0.4 μm + 10 × 0.2 μm + 5 × 0.1 μm
87/5/8	188 ± 6	2 × 0.4 μm + 10 × 0.2 μm + 5 × 0.1 μm
85/5/10	195 ± 6	2 × 0.4 μm + 10 × 0.2 μm + 10 × 0.1 μm
EPC/PA/Chol:		
86/5/9	180 ± 3	2 × 0.4 μm + 15 × 0.2 μm
79/5/16	179 ± 4	2 × 0.4 μm + 15 × 0.2 μm
72/5/23	185 ± 3	2 × 0.4 μm + 15 × 0.2 μm
65/5/30	190 ± 5	2 × 0.4 μm + 15 × 0.2 μm

[a] Mean ± SD from 3–4 determinations.

$$a_2 = -\frac{V_s}{2.303RT}(\delta_2 - \delta_{EPC})^2 \quad (12)$$

and f_{EPC} and V_{EPC} are, respectively, the solute permeability decrement and the effective molar volume in EPC-only membranes. These equations, which provide a theoretical basis for describing quantitatively the effects of different concentrations of various membrane components on solute permeability across biomembranes, were utilized to model the experimental permeabilities obtained in this study.

Results and Discussion

Effects of gA or Chol Concentration on Permeability

To minimize possible effects of membrane surface curvature on solute permeability (Brunner et al., 1980), large unilamellar vesicles having similar hydrodynamic diameters were prepared. Due to the varying rigidity of membranes containing different concentrations of gramicidin A or cholesterol, extrusion through various combinations of different pore-size polycarbonate filters (0.4, 0.2 and/or 0.1 μm) was required, as described in Table 1. Table 1 also lists the hydrodynamic diameters obtained by dynamic light scattering, demonstrating that it was possible to obtain hydrodynamic diameters within a narrow range of 170–200 nm using these extrusion sequences.

Gramicidin A was added from ethanolic solution, which has been shown to result in the incorporation of gA into membranes in a predominantly nonchannel con-

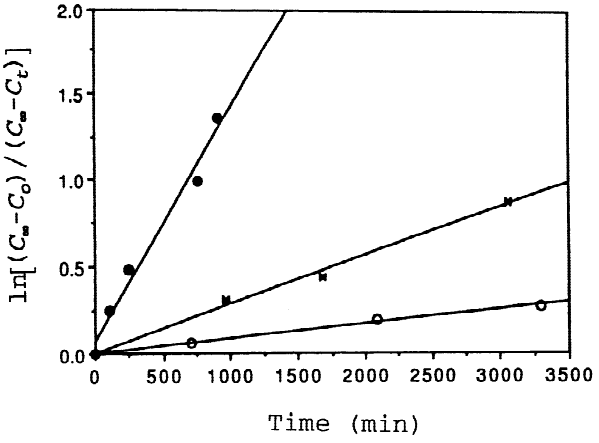

Fig. 1. Representative flux profiles for α-carbamoyl-*p*-methyl-hippuric acid (CMHA) across EPC membranes at 25°C. Key: (●), in the presence of 10 mol% gramicidin A (pH = 6.55); (○) in the presence of 23 mol% cholesterol (pH = 6.49); and (**x**), in the absence of both gA and Chol (pH = 6.49).

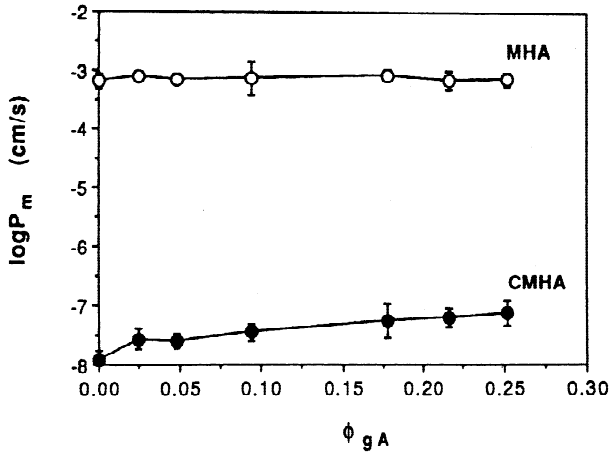

Fig. 2. Log of the permeability coefficients, P_m, for CMHA (●) and MHA (○) as a function of the volume fraction of gA (φ_{gA}) in EPC membranes.

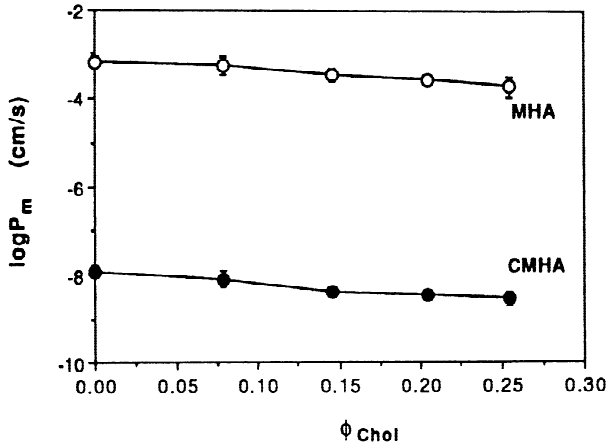

Fig. 3. Log of the permeability coefficients, P_m, for CMHA (●) and MHA (○) as a function of the mole fraction of Chol (φ_{Chol}) in EPC membranes.

formation (Muller et al., 1995). However, nonchannel gramicidin A is known to undergo a transition to a channel conformation at elevated temperatures (Cox et al., 1992), which is followed by a transition to an H_{II} nonlamellar phase. Vesicle fusion and leakage subsequent to this transition may affect permeability measurements. Fortunately, Muller et al. (1995) noted that the dilution and unilamellarity of vesicles make vesicle fusion due to a transition to the H_{II} phase highly improbable. Since fusion of liposomes into larger vesicles and/or the formation of vesicle aggregates would lead to significant changes of vesicle hydrodynamic diameter, we monitored vesicle size after the addition of 10 mol% gramicidin A in EPC/PA membranes using dynamic light scattering. Although occasional large changes of vesicle size were observed after prolonged incubation, most of the vesicle samples prepared were stable over the time frame of the transport experiments. Moreover, circular dichroism measurements reported in a previous paper by the authors (Xiang & Anderson, 2000) indicated that the nonchannel conformation of gA was retained over a 10-day period in EPC membranes.

Figure 1 shows representative flux profiles for α-carbamoyl-*p*-methyl-hippuric acid (CMHA) across EPC membranes in the presence and absence of 10 mol% gramicidin A or 23 mol% Chol. Rate constants (k_{obs}) were obtained from linear least-squares fits of the data in Fig. 1 according to Eq. 1. Solute permeability coefficients (P_m) were then determined according to Eq. 2 by inputting the hydrodynamic diameter and pH corresponding to a given k_{obs}.

The permeability coefficients obtained for CMHA and unsubstituted *p*-methyl-hippuric acid (MHA) are plotted in Figs. 2 and 3, respectively, as a function of the volume fraction, φ_2, of gA or Chol in EPC membranes. Volume fractions were calculated from the mole fraction x_2 and molar volume V_2 for gA or Chol and the molar volume V_1 for EPC as follows

$$\varphi_2 = \frac{x_2 V_2}{(1-x_2)V_1 + x_2 V_2} \tag{13}$$

Biomembranes are heterogenous along the direction normal to the bilayer surface with each region (i.e., the headgroup and acyl chain regions) exhibiting distinctly different barrier properties (Marrink & Berendsen, 1996). Our previous experimental studies (Xiang & Anderson, 1994; Xiang et al., 1992) and molecular dynamics studies by Marrink and Berendsen (1996) have shown that the barrier domain in liquid-crystalline membranes resides in the highly-ordered acyl chain region.

Table 2. Physicochemical properties of solutes and membrane components in the barrier domain

Solute or membrane component	pK_a	Molar volume[c] (ml/mol)	Solubility parameters $(cal/ml)^{1/2}$
p-Methyl-hippuric acid	3.85[a]	140.0	13.2[c]
α-Carbamoyl-*p*-methyl-hippuric acid	3.70[a]	140.1	15.7[c]
Gramicidin A	NA[b]	1252[d]	13.8[c] (13.2[e])
Egg lecithin	NA[b]	423[d]	8.32[c,d]
Cholesterol	NA[b]	371[d]	8.70[c,d] (7.7[e])

[a] From (Mayer et al., 2000); [b]not applicable; [c]estimated from the method of Fedors (1974); [d]in the nonpolar acyl chain region where the transport barrier resides (Xiang & Anderson, 1994); [e]obtained from permeability results for CMHA and MHA (this study).

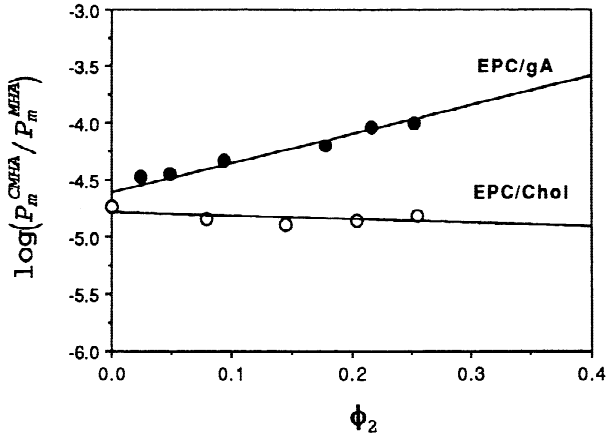

Fig. 4. Logarithm of the ratio of P_m values for CMHA and MHA as a function of the volume fraction (φ_2) of gA (●) or Chol (○) in EPC membranes.

EPC molecules are comprised of two acyl chains with an average of one double bond per chain and an average chain length of 18 carbon segments, about 70% of which constitutes the highly ordered region. Chol also resides in the acyl chain region with the exception of its hydroxyl group which anchors Chol in the headgroup interfacial region. Gramicidin A forms a double-helical head-to-tail dimer in a nonchannel conformation, which spans the entire length of the acyl chain region. Molar volumes needed in Eq. 13 and solubility parameters were calculated for gA, the portion of Chol that resides in the acyl chain region, and the highly ordered acyl chains in EPC using the method of Fedors (1974), which is based on the additivity principle for atomic and group contributions to the energy of vaporization and molar volume. This method has been widely used to estimate molecular solubility parameters (Bustamante & Selles, 1986; Lin, Wang & Huang, 1991). The calculated results, presented in Table 2, indicate that the solubility parameters corresponding to the nonpolar regions of EPC and Chol are very close to each other (8.3 *vs.* 8.7 $(cal/ml)^{1/2}$), suggesting that the effects of Chol on membrane permeability may arise mainly from its ordering effects on biomembranes.

As shown in Fig. 2, the P_m for CMHA increases by a factor of 6.0 ± 1.8 over the gA concentration range employed while P_m for the more lipophilic, unsubstituted permeant, MHA, remains almost unchanged. These results are in sharp contrast to those in Chol-containing membranes shown in Fig. 3 where the permeability coefficients for both CMHA and MHA decrease by similar factors of 4.2 ± 1.1 and 3.5 ± 1.2, respectively. Thus, changes in solute permeability with transmembrane peptide content depend on permeant lipophilicity, while permeability changes resulting from cholesterol incorporation appear to be independent of permeant lipophilicity. Since both gA and Chol order EPC membranes (*vida infra*), the effects of membrane ordering alone cannot explain these observations. It is thus necessary to investigate the effects of changes in both membrane hydrophobicity and order as a function of gA and Chol composition.

Effects of Membrane Hydrophobicity on Permeability

As shown in Table 2, CMHA and MHA are very similar in molecular size. As a result, the appropriate value of the permeability decrement, f_m, necessary to correct for the effects of bilayer chain ordering on the transport of these two solutes as defined in Eqs. 8 and 9 should be identical. Thus, the different changes in $\log P_m$ values for CMHA and MHA must originate from the effects of gA or Chol on membrane hydrophobicity. Using regular solution theory as formulated in Eq. 6, we have

$$\log(P_m^{CMHA}/P_m^{MHA}) = \log(P_{EPC}^{CMHA}/P_{EPC}^{MHA}) + \frac{2V_s}{2.303RT}(\delta_2 - \delta_{EPC})(\delta_{CMHA} - \delta_{MHA})\varphi_2 \quad (14)$$

where P_{EPC} is the permeability coefficient of solute across an EPC-only membrane. The logarithm of the ratio of P_m values for CMHA and MHA is a linear function of the volume fraction φ_2 of gA or Chol in EPC membranes with a slope that depends on the differences in the solubility parameters between the two membrane components (δ_{EPC} and δ_2) and between the two permeants (δ_{CMHA} and δ_{MHA}). Figure 4 shows the logarithm of the ratio of P_m values for CMHA and MHA as a function of the volume fraction φ_2 of gA or Chol. Remarkably, while $\log [P_m^{CMHA}/P_m^{MHA}]$ is virtually unchanged with varying Chol concentration in EPC mem-

branes, it increases substantially with increasing gA concentration. Since CMHA has an extra amide group, the increase in log $[P_m^{CMHA}/P_m^{MHA}]$ reflects a more favorable electrostatic interaction for CMHA in gA-containing membranes. Least-squares fits of the data in Fig. 4 yielded slopes for the gA and Chol-containing membranes of 2.5 ± 0.3 and −0.3 ± 0.3, respectively. Using the method of Fedors (1974), solubility parameters (δ_s) for CMHA and MHA were calculated to be 15.7 and 13.2 $(cal/ml)^{1/2}$, respectively, while their molar volumes (V_s) were estimated to be 140 ml/mol. Combining all these results, solubility parameters for gA and Chol of $\delta_{gA} = 13.2$ and $\delta_{Chol} = 7.7$ $(cal/ml)^{1/2}$, respectively, were obtained from Eq. 14. Apparently, the greater increase in P_m^{CMHA} over P_m^{MHA} in gA-containing membranes can be accounted for by an increase in membrane solubility parameter (δ_m) due to the larger value of δ_{gA} in comparison to δ_{EPC}. The structural factors that determine the solubility parameter of gA include the dispersion interactions, polar interactions, and hydrogen-bonding interactions as described by the following empirical equation (Hansen & Beerbower, 1971; Hoy & Martin, 1975):

$$\delta_{gA}^2 = \delta_d^2 + \delta_p^2 + \delta_h^2 \qquad (15)$$

where δ_d, δ_p, and δ_h are the partial solubility parameters due to dispersion, polar, and hydrogen bonding interactions in gA. If the dispersion interactions for both gA and EPC are similar, the larger effective δ_{gA} value may arise from the additional contributions of polar and hydrogen-bonding functional groups to the solubility parameter of gA. The increase of δ_m in the presence of gA thus reflects a more hydrophilic environment in the membrane interior.

The method of Fedors (1974) was also used to estimate the solubility parameter for gA, which requires only a knowledge of the chemical structure of the amino acid residues in gA. The δ_{gA} value so obtained is 13.8 $(cal/ml)^{1/2}$, close to the value (13.2 $(cal/ml)^{1/2}$) obtained from Eq. 14. This may be fortuitous, however, since the individual contributions of the amino acid residues considered in isolation are likely to be altered due to the double-helical secondary structure for nonchannel gA and the ordering and relative immobility of the peptide in the membranes. Nevertheless, the large δ_{gA} value obtained supports our earlier assertion that the effective transport pathway is more hydrophilic due to the presence of the transmembrane peptide gA (Xiang & Anderson, 2000). It is also possible that the more polar CMHA preferentially permeates within a region nearer to the lipid-gramicidin interface.

The slightly smaller δ_{Chol} (7.7 ± 0.6 $(cal/ml)^{1/2}$) in comparison to δ_{EPC} (8.3 $(cal/ml)^{1/2}$), though not statistically significant, may arise from the higher degree of saturation and rigidity in Chol than in egg lecithin making van der Waals interactions for permeating solutes in Chol-containing membranes less favorable. Indeed, intercalation of Chol in lipid membranes has been known to decrease the depth of water penetration in lipid membranes by about 2.5 Å (Simon et al., 1982; Perochon, Lopez & Tocanne, 1992). A slight increase of hydrophobicity in the interior of DOPC and EPC membranes in the presence of 30 mol% Chol has also been observed in a previous ESR study (Subczynski et al., 1994). However, the present results suggest that these effects, if any, are minor in comparison to the Chol induced chain ordering effects on membrane permeability (*vida infra*). This is consistent with recent findings in the authors' laboratory that the presence of 50 mol% Chol in phospholipid membranes shifts the effective barrier domain hydrophobicity from decadiene-like to an environment resembling hexadecene, a slightly more hydrophobic solvent (Xiang et al., 1998).

Effects of Gramicidin A on Membrane Hydrophobicity

Changes in membrane hydrophobicity in the presence of gramicidin A were also investigated by monitoring the fluorescence lifetime of 12-(9-anthroyloxyl)-stearic acid (12-ANS) incorporated into bilayer membranes as a function of added gA. This probe is known to reside well within the ordered acyl chain region of the bilayer (Podo & Blasie, 1977), which is the barrier domain for solute permeation, and is well suited to examine changes of barrier hydrophobicity in the presence of gramicidin A as a result of its well-defined location within the bilayer and the sensitivity of its fluorescence lifetime to the hydrogen-bond donating capacity of the surrounding medium and to relatively polar tryptophan residues located in close proximity (Perochon et al., 1992; Garrison et al., 1994). Figure 5 shows the mean lifetime and long and short lifetime components of 12-ANS as a function of gA concentration in EPC membranes. Analyses of the fluorescence data indicated that the fluorescence decay can be best described as biexponential both in the membranes and in hexadecane, in agreement with previous studies in viscous paraffins and lipid bilayers (Matayoshi & Kleinfeld, 1981). The long lifetime component dominates the fluorescence decay with a fraction of >0.9. As illustrated in Fig. 5, the mean and long lifetimes decrease significantly (>20%) with increasing gA concentration. The fluorescence lifetime for 12-ANS is sensitive to solvent viscosity (Matayoshi & Kleinfeld, 1981). For example, the mean lifetime for 12-ANS in low-viscosity hexane is 7.3 ns (Garrison et al., 1994) while the present measurements and studies by Matayoshi et al. (1981) yielded mean lifetimes of 9.3 ns and 11 ns in the more viscous solvents, hexadecane and paraffin oil, respectively. This trend is opposite to that observed in the lipid

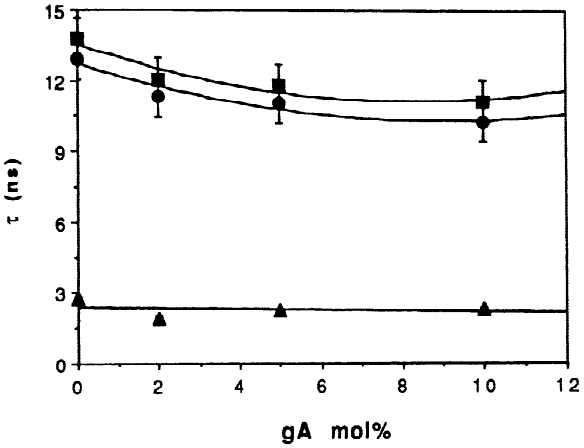

Fig. 5. The average lifetime and the two lifetime components for the fluorescence of 12-ANS in EPC vesicles versus the mole fraction of membrane-incorporated gramicidin A. Key: (●), average lifetime; (■), long lifetime component; and (▲), short-lifetime component.

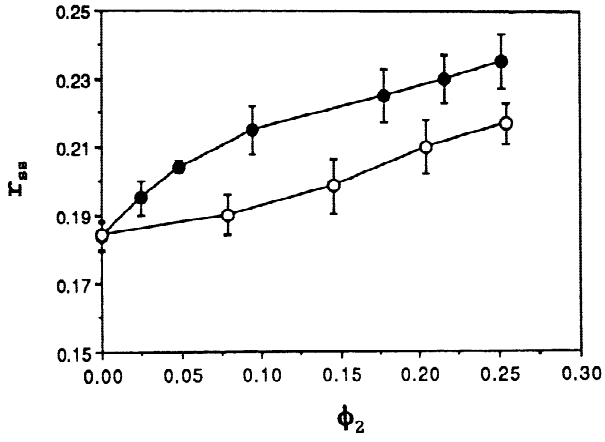

Fig. 6. Steady-state fluorescence anisotropy values, r_{ss}, for TMA-DPH in EPC membranes as a function of the volume fraction, φ_2, of gA (●) or Chol (○) in EPC membranes.

membranes, however, where the mean lifetime of 12-ANS decreases with the gA concentration in the membranes even though the presence of gramicidin A was found to decrease membrane fluidity as measured by the fluorescence anisotropy of TMA-DPH (*vida infra*). Had this viscosity effect been absent, the reduction of the lifetime for 12-ANS in the peptide-containing membranes might have been more substantial.

Three factors may be responsible for the reduction of the fluorescence lifetime for 12-ANS. First, due to thermal fluctuations in the peptide conformation, a fraction of the hydrogen-bonding groups such as amide bonds in gA may be accessible within the nonpolar acyl chain region. Applying multiple linear regression analysis to the observed Stokes' shift, Garrison and coworkers (1994) found that the fluorescence properties of 9-anthroyloxy fatty acids are sensitive to the hydrogen-bond donating capacity of the solvent but are not affected by the hydrogen-bond accepting capacity. Indeed, the lifetime for 6-ANS in hexane is reduced from 7.8 ns to 6.0 ns upon the addition of a small amount of ethanol (1% v/v), a hydrogen-bond donating solvent, while it is actually increased in ethyl acetate, a polar, hydrogen-accepting solvent (Garrison et al., 1994). Second, water molecules penetrate deeper into the acyl chain region in the presence of the relatively hydrophilic transmembrane peptide. Third, the fluorescence may be quenched by relatively polar tryptophan residues in gramicidin A as suggested by the decrease of the fluorescence intensity for n-(9-anthroyloxy) fatty acids (n = 2, 6, 9, and 12) in gA-containing DMPC membranes (Haigh, Thulborn & Sawyer, 1979), though these residues reside mainly near the surface of the membranes and the quenching efficiency is the lowest for 12-(9-anthroyloxy) fatty acids. At present, the exact mechanism(s) cannot be established. However, all of these factors may lead to an increase in the barrier domain polarity, consistent with the increased value for the membrane solubility parameter in the presence of the transmembrane peptide, gA.

Effects of Membrane Order on Permeability

Figure 6 shows the steady-state anisotropy (r_{ss}) for TMA-DPH as a function of the volume fraction (φ_2) of gA or Chol in EPC membranes. TMA-DPH has a positively charged trimethylamino headgroup and is thereby tethered to the bilayer surface and oriented, on average, normal to the membrane interface. The steady-state anisotropy of TMA-DPH is known to primarily reflect lipid ordering in biomembranes because of the approximately collinear excitation/emission dipoles with respect to the long molecular axis in TMA-DPH (Engel & Prendergast, 1981). This is supported by a high correlation (r = 0.97) between the order parameters (S_f) for TMA-DPH estimated from the corresponding r_{ss} values and lipid segmental order parameters (S_m) in the plateau region obtained from ^{2}H-NMR in various lipid membranes (Xiang et al., *unpublished results*). Thus, similar r_{ss} values for TMA-DPH indicate similar lipid chain order. As shown in Fig. 6, both gA and Chol increase chain ordering within lipid membranes with gA demonstrating a more substantial increase of r_{ss} at a given volume fraction. Using Raman spectroscopy and calorimetry, Chapman et al. (1977) found that the action of gramicidin on chain order is similar to that of cholesterol in that both decrease the number of *gauche* conformers in liquid-crystalline bilayers.

From Eqs. 10–12, one can evaluate the ordering effects of gA or Chol on the solute permeability decrement (f_m) from changes in solute permeability coefficients with the concentration of gA or Chol in the membranes

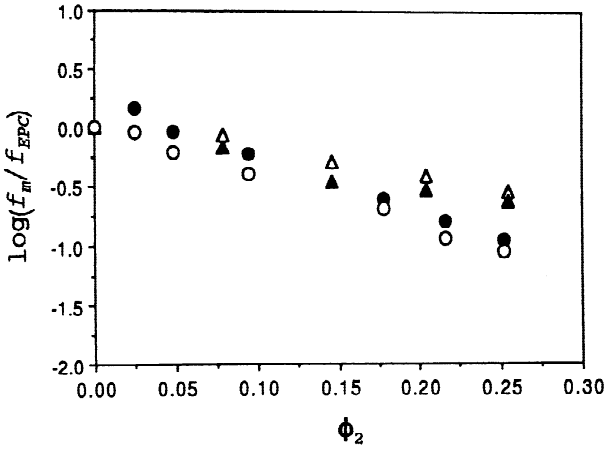

Fig. 7. Logarithm of the ratio f_m/f_{EPC} as a function of the volume fraction, φ_2, of gA or Chol in EPC membranes. Key: CMHA (●) and MHA (○) in gA-containing membranes; and CMHA (▲) and MHA (△) in Chol-containing membranes.

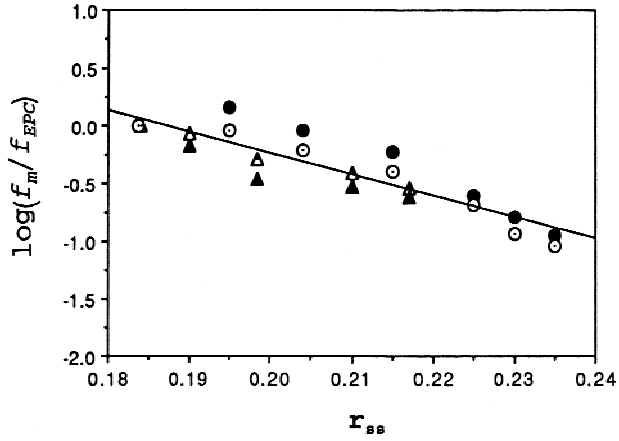

Fig. 8. Logarithm of the ratio f_m/f_{EPC} as a function of the fluorescence anisotropy, r_{ss}, for TMA-DPH. Key: CMHA (●) and MHA (○) in gA-containing membranes; and CMHA (▲) and MHA (△) in Chol-containing membranes.

and the permeant and membrane constituent solubility parameters obtained above. The results for the logarithm of the ratio of f_m in either gA or Chol-containing membranes relative to f_{EPC} in EPC-only membranes are presented in Fig. 7. Both transmembrane gA and Chol reduce f_m with the effect being more pronounced when gA is the ordering agent, consistent with the separate experimental results for the steady-state anisotropy (r_{ss}) of TMA-DPH in gA *vs.* Chol-containing EPC membranes (Fig. 6).

The dependence of the permeability decrement, f_m, on fluorescence anisotropy, r_{ss}, of TMA-DPH in both gA and Chol-containing EPC membranes is shown in Fig. 8. Although the data points do not appear to be entirely randomly distributed about the fitted line, which may result in part from the experimental uncertainties and model approximations, the linear fits of the four data sets for two different solutes (CMHA and MHA) in different membranes (gA and Chol-containing membranes) yield slopes in a narrow range of −17 to −22. A least-squares fit of all the data points yields a slope and intercept of -18.6 ± 1.8 and 3.48 ± 0.37 ($r = 0.91$), respectively, suggesting that, as a first approximation, f_m can be modeled as a universal function of membrane order as characterized here by fluorescence anisotropy for TMA-DPH, regardless of the nature of the ordering agent. Strong correlations between permeability coefficients for small molecules (e.g., water, acetamide and urea) and fluorescence anisotropy values for membrane-bound DPH have also been found in model lipid membranes varying in Chol, sphingomyelin content and acyl chain saturation (Lande et al., 1995), leading to the suggestion that the barrier function of several epithelia such as renal collecting duct, urinary bladder, and gastric mucosa may be due to the low fluidity of the apical membranes of these epithelia. Indeed, as shown in Fig. 7 or 8, the change in permeability decrement due to membrane ordering exceeded an order of magnitude over the concentration ranges for gA and Chol employed in this study.

Conclusions

In summary, a quantitative approach has been developed to model the dependence of solute permeability on the concentrations of a transmembrane peptide, gramicidin A, and cholesterol in lipid bilayer membranes. The effects of these membrane components on solute permeability can be rationalized in terms of their independent contributions to bilayer chain ordering and barrier domain hydrophobicity. The ordering and hydrophobicity effects have been modeled, respectively, in the framework of free-surface-area theory and regular solution theory using membrane order parameters and solubility parameters as indices to describe changes in lipid packing and barrier domain hydrophobicity in membranes varying in gA or Chol concentration. This combined theoretical model satisfactorily accounts for the transport results for α-carbamoyl-*p*-methylhippuric acid and the unsubstituted *p*-methylhippuric acid, two permeants with similar molecular size but markedly different lipophilicity. Thus, transmembrane gA in its nonchannel conformation increases the permeability of the more hydrophilic permeant, CMHA, but has no influence on MHA. Transmembrane gA decreases the hydrophobicity of the barrier domain while increasing chain ordering. The balance of these changes may result in enhancement or inhibition of permeability depending on permeant lipophilicity and size. The permeabilities of both model permeants decrease with added Chol due mainly to the ordering effects of Chol in lipid membranes. These dis-

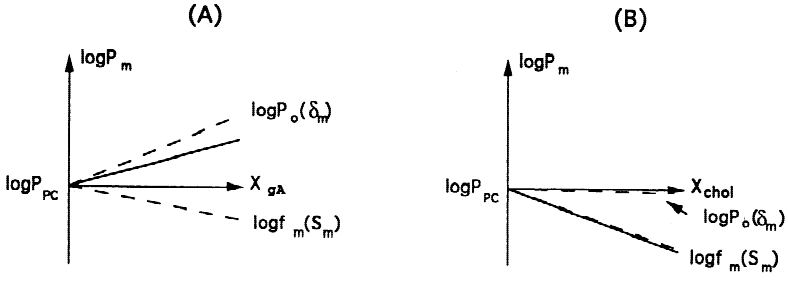

Fig. 9. A schematic depiction of the effects of transmembrane peptides (panel *A*) and Chol (panel *B*) on solute permeability, P_m, across biomembranes. The solid lines represent the net effects of changes in membrane order and hydrophobicity ($K_{PC\rightarrow m}(\delta_m)$ and $f_m(S_m)$, respectively) on solute permeability.

tinct behaviors of a transmembrane peptide and cholesterol and their effects on solute permeability are depicted in Fig. 9. More studies will be undertaken to apply the quantitative permeability model developed here to other membranes in order to understand how solute permeability and membrane hydrophobicity vary with the chemical nature and conformation of various transmembrane proteins.

This work was supported by a grant from the National Institutes of Health (RO1 GM51347). The authors would like to thank Dr. James Herron, University of Utah, for his assistance with the fluorescence polarization experiments which were performed in his laboratory.

References

Anderson, O.S. 1984. Gramicidin channels. *Annu. Rev. Physiol.* **46:**531–548

Bartlett, G.R. 1959. Colorimetric assay methods for free and phosphorylated glyceric acids. *J. Biol. Chem.* **234:**469–471

Brunner, J., Graham, D.E., Hauser, H., Semenza, G. 1980. Ion and sugar permeabilities of lecithin bilayers: comparison of curved and planar bilayers. *J. Membrane Biol.* **57:**133–141

Bustamante, P., Selles, E. 1986. Relationship between the solubility parameter and the binding of drugs by plasma proteins. *J. Pharm. Sci.* **75:**639–643

Carruthers, A., Melchior, D.L. 1983. Studies of the relationship between bilayer water permeability and bilayer physical state. *Biochemistry* **22:**5797–5807

Cevc, G., Seddon, J.M., Harttung, R., Eggert, W. 1988. Phosphatidylcholine-fatty acid membranes. I. Effects of protonation, salt concentration, temperature and chain length on the colloidal and phase properties of mixed vesicles, bilayers and nonlamellar structures. *Biochem. Biophys. Acta* **940:**219–240

Chan, T.C. 1983. Diffusion of pseudospherical molecules: An investigation on the effects of dipole moment. *J. Phys. Chem.* **79:**3591–3593

Chapman, D., Cornell, B.A., Eliasz, A.W., Perry, A. 1977. Interactions of helical polypeptide segments which span the hydrocarbon region of lipid bilayers. Studies of the gramicidin A lipid-water system. *J. Mol. Biol.* **113:**517–538

Clerc, S.G., Thompson, T.E. 1995. Permeability of dimyristoyl phosphatidylcholine/dipalmitoyl phosphatidylcholine bilayer membranes with coexisting gel and liquid-crystalline phases. *Biophys. J.* **68:**2333–2341

Cornell, B. 1987. Gramicidin A-phospholipid model systems. *J. Bioenerg. Biomembr.* **19:**655–676

Cox, K.J., Ho, C., Lombardi, J.V., Stubbs, C.D. 1992. Gramicidin conformational studies with mixed-chain unsaturated phospholipid bilayer systems. *Biochemistry* **31:**1112–1118

Daum, G. 1985. Lipids of mitochondria. *Biochim. Biophys. Acta* **822:**1–42

DeYoung, L.R., Dill, K.A. 1988. Solute partitioning into lipid bilayer membranes. *Biochemistry* **27:**5281–5289

Diamond, J.M., Katz, Y. 1974. Interpretation of nonelectrolyte partition coefficients between dimyristoyl lecithin and water. *J. Membrane Biol.* **17:**121–154

Engel, L.W., Prendergast, F.G. 1981. Values for and significance of order parameters and "cone angles" of fluorophore rotation in lipid bilayers. *Biochemistry* **20:**7338–7345

Fedors, R.F. 1974. A method for estimating both the solubility parameters and molar volumes of liquids. *Polym. Eng. Sci.* **14:**147–154

Finkelstein, A. 1976. Water and nonelectrolyte permeability of lipid bilayer membranes. *J. Gen. Physiol.* **68:**127–135

Garrison, M.D., Doh, L.M., Potts, R.O., Abraham, W. 1994. Fluorescence spectroscopy of 9-anthroyloxy fatty acids in solvents. *Chem. Phys. Lipids* **70:**155–162

Grant, D.J.W., Higuchi, T. 1990. Solubility Behavior of Organic Compounds. John Wiley & Sons, New York

Griffith, O.H., Dehlinger, P.J., Van, S.P. 1974. Shape of the hydrophobic barrier of phospholipid bilayers (evidence for water penetration in biological membranes). *J. Membrane Biol.* **15:**159–192

Haigh, E.A., Thulborn, K.R., Sawyer, W.H. 1979. Comparison of fluorescence energy transfer and quenching methods to establish the position and orientation of components within the transverse plane of the lipid bilayer. Application to the gramicidin A-bilayer interaction. *Biochemistry* **18:**3525–3532

Hansen, C., Beerbower, A. 1971. Solubility parameters. *In:* Kirk-Othmer Encyclopedia of Chemical Technology. A. Standen, editor. Wiley, New York

Hauser, H., Howell, K., Dawson, R.M.C., Bowyer, D.E. 1980. Rabbit small intestinal brush border membrane. Preparation and lipid composition. *Biochim. Biophys. Acta* **602:**567–577

Haydon, D.A., Hladky, S.B. 1972. Ion transport across thin lipid membranes: A critical discussion of mechanisms in selected systems. *Quart. Rev. Biophys.* **5:**187–282

Hildebrand, J.H., Scott, R.L. 1950. The Solubility of Nonelectrolytes. Reinhold Publishing, New York

Hoy, K.L., Martin, R.A. 1975. Tables of Solubility Parameters. Union Carbide, New York

Killian, J.A. 1992. Gramicidin and gramicidin-lipid interactions. *Biochim. Biophys. Acta* **1113:**391–425

Koeppe, R.E., Killian, J.A., Greathouse, D.V. 1994. Orientations of the tryptophan 9 and 11 side chains of the gramicidin channel based on deuterium nuclear magnetic resonance spectroscopy. *Biophys. J.* **66:**14–24

Lande, M.B., Donovan, J.M., Zeidel, M.L. 1995. The relationship between membrane fluidity and permeabilities to water, solutes, ammonia, and protons. *J. Gen. Physiol.* **106:**67–84

Lentz, B.R. 1993. Use of fluorescent probes to monitor molecular order and motions within liposome bilayers. *Chem. Phys. Lipids* **64:**99–116

Levin, V.A. 1980. Relationship of octanol/water partition coefficient and molecular weight to rat brain capillary permeability. *J. Med. Chem.* **23:**682–684

Lin, H., Wang, Z., Huang, C. 1991. The influence of acyl chain-length asymmetry on the phase transition parameters of phosphatidylcholine dispersions. *Biochim. Biophys. Acta* **1067:**17–28

Marrink, S.J., Berendsen, H.J.C. 1994. Simulation of water transport through a lipid membrane. *J. Phys. Chem.* **98:**4155–4168

Marrink, S.J., Berendsen, H.J.C. 1996. Permeation process of small molecules across lipid membranes studied by molecular dynamics simulations. *J. Phys. Chem.* **100:**16729–16738

Matayoshi, E.D., Kleinfeld, A.M. 1981. Emission wavelength-dependent decay of the 9-anthroyloxy-fatty acid membrane probes. *Biophys. J.* **35:**215–235

Mayer, P., Xiang, T.-X., Anderson, B.D. Independence of substituent contributions to the transport of small molecule permeants in lipid bilayers. *AAPS PharmSci.* **2:** article 14 (http://www.pharmsci.org/)

Muller, J.M., van Ginkel, G., van Faassen, E.E. 1995. Effect of gramicidin A on structure and dynamics of lipid vesicle bilayers. A time-resolved fluorescence depolarization study. *Biochemistry* **34:**3092–3101

Nagle, J.F. 1993. Area/lipid of bilayers from NMR. *Biophys. J.* **64:**1476–1481

Paula, S., Volkov, G., Deamer, D.W. 1998. Permeation of halide anions through phospholipid bilayers occurs by the solubility-diffusion mechanism. *Biophys. J.* **74:**319–327

Perochon, E., Lopez, A., Tocanne, J.F. 1992. Polarity of lipid bilayers. A fluorescence investigation. *Biochemistry* **31:**7672–7682

Podo, F., Blasie, J.K. 1977. Nuclear magnetic resonance studies of lecithin bimolecular leaflets with incorporated fluorescent probes. *Proc. Natl. Acad. Sci. USA* **74:**1032–1036

Rapoport, S.I., Ohno, K., Pettigrew, K.D. 1979. Drug entry into the brain. *Brain Res.* **172:**354–359

Seelig, A., Seelig, J. 1974. The dynamic structure of fatty acyl chains in a phospholipid bilayer measured by deuterium magnetic resonance. *Biochemistry* **13:**4839–4845

Simon, S.A., McIntosh, T.J., Latorre, R. 1982. Influence of cholesterol on water penetration into bilayers. *Science* **216:**65–66

Singer, S.J., Nicolson, G.L. 1972. The fluid mosaic model of the structure of cell membranes. *Science* **175:**720–731

Stockton, G.W., Smith, I.C.P. 1976. A deuterium nuclear magnetic resonance study of the condensing effect of cholesterol on egg phosphatidylcholine bilayer membranes. *Chem. Phys. Lipids* **17:**251–263

Subczynski, W.K., Wisniewska, A., Yin, J.-J., Hyde, J.S., Kusumi, A. 1994. Hydrophobic barriers of lipid bilayer membranes formed by reduction of water penetration by alkyl chain unsaturation and cholesterol. *Biochemistry* **33:**7670–7681

Wallace, B.A. 1990. Gramicidin channels and pores. *Annu. Rev. Biophys Biophys. Chem.* **19:**127–157

Walter, A., Gutknecht, J. 1986. Permeability of small nonelectrolytes through lipid bilayer membranes. *J. Membrane Biol.* **90:**207–217

Xiang, T.-X., Anderson, B.D. 1994. Substituent contributions to the permeability of substituted *p*-toluic acids in lipid bilayer membranes. *J. Pharm. Sci.* **83:**1511–1518

Xiang, T.-X., Anderson, B.D. 1995. Development of a combined NMR paramagnetic ion-induced line-broadening/dynamic light scattering method for permeability measurements across lipid bilayer membranes. *J. Pharm. Sci.* **84:**1308–1315

Xiang, T.-X., Anderson, B.D. 1997. Permeability of acetic acid across gel and liquid-crystalline lipid bilayers conforms to free-surface-area theory. *Biophys. J.* **72:**223–237

Xiang, T.-X., Anderson, B.D. 1998. Influence of chain ordering on the selectivity of dipalmitoylphosphatidylcholine bilayer membranes for permeant size and shape. *Biophys. J.* **75:**2658–2671

Xiang, T.-X., Anderson, B.D. 2000. Influence of a transmembrane protein on the permeability of small molecules across lipid membranes. *J. Membrane Biol.* **173:**187–201

Xiang, T.-X., Chen, X., Anderson, B.D. 1992. Transport methods for probing the barrier domain of lipid bilayer membranes. *Biophys. J.* **63:**78–88

Xiang, T.-X., Xu, Y.-H., Anderson, B.D. 1998. The barrier domain for solute permeation varies with lipid bilayer phase structure. *J. Membrane Biol.* **165:**77–90

Yeagle, P. 1992. The Structure of Biological Membranes. CRC Press, Boca Raton